TRAUMA SURGERY

Angulated locking plate in periprosthetic proximal femur fractures: biomechanical testing of a new prototype plate

**Mark Lenz · Boyko Gueorguiev · Steve Joseph · Bas van der Pol ·
Robert Geoff Richards · Markus Windolf · Karsten Schwieger · Piet de Boer**

Abstract

Introduction To improve proximal plate fixation of periprosthetic femur fractures, a prototype locking plate with proximal posterior angulated screw positioning was developed and biomechanically tested.

Methods Twelve fresh frozen, bone mineral density matched human femora, instrumented with cemented hip endoprosthesis were osteotomized simulating a Vancouver B1 fracture. Specimens were fixed proximally with monocortical (LCP) or angulated bicortical (A-LCP) head-locking screws. Biomechanical testing comprised quasi-static axial bending and torsion and cyclic axial loading until catastrophic failure with motion tracking.

Results Axial bending and torsional stiffness of the A-LCP construct were (1,633 N/mm ± 548 standard deviation (SD); 0.75 Nm/deg ± 0.23 SD) at the beginning and (1,368 N/mm ± 650 SD; 0.67 Nm/deg ± 0.25 SD) after 10,000 cycles compared to the LCP construct (1,402 N/mm ± 272 SD; 0.54 Nm/deg ± 0.19 SD) at the beginning and (1,029 N/mm ± 387 SD; 0.45 Nm/deg ± 0.15) after 10,000 cycles. Relative movements for medial bending and axial translation differed significantly between the constructs after 5,000 cycles (A-LCP 2.09° ± 0.57 SD; LCP 5.02° ± 4.04 SD; $p = 0.02$; A-LCP 1.25 mm ± 0.33 SD; LCP 2.81 mm ± 2.32 SD; $p = 0.02$) and after 15,000 cycles (A-LCP 2.96° ± 0.70; LCP 6.52° ± 2.31; $p = 0.01$; A-LCP 1.68 mm ± 0.32; LCP 3.14 mm ± 0.68; $p = 0.01$). Cycles to failure (criterion 2 mm axial translation) differed significantly between A-LCP (15,500 ± 2,828 SD) and LCP construct (5,417 ± 7,236 SD), $p = 0.03$.

Conclusion Bicortical angulated screw positioning showed less interfragmentary osteotomy movement and improves osteosynthesis in periprosthetic fractures.

M. Lenz (✉) · B. Gueorguiev · B. van der Pol ·
R. G. Richards · M. Windolf · K. Schwieger
AO Research Institute Davos, Clavadelerstrasse 8,
7270 Davos-Platz, Switzerland
e-mail: mark.lenz@aofoundation.org

B. Gueorguiev
e-mail: boyko.gueorguiev@aofoundation.org

B. van der Pol
e-mail: b.vanderpol@signus-med.de

R. G. Richards
e-mail: geoff.richards@aofoundation.org

M. Windolf
e-mail: markus.windolf@aofoundation.org

K. Schwieger
e-mail: karsten.schwieger@aofoundation.org

S. Joseph
Department of Orthopaedics, York Hospital,
Wigginton Road, York, North Yorkshire YO31 8HE, UK
e-mail: steve.joseph@york.nhs.uk

P. de Boer
Department of Anatomy, Hull and York Medical School,
York, UK
e-mail: piet.deboer@aofoundation.org

Introduction

The treatment of periprosthetic femur fractures is becoming much more important due to the increasing number of total hip arthroplasties (THA). Such fractures occur during implantation in 1 % of the cemented and in 3–18 % of the uncemented primary THAs, respectively [1]. In almost all

cases, elderly patients are affected, so fixation permitting early full weight bearing is desirable to avoid prolonged immobilization and bed rest. The quality of the bone stock is often poor due to postmenopausal or age-related osteoporosis. The introduction of uncemented press-fit stems has substantially increased intraoperative fracture rates [2]. Unfortunately, bone defects generated during THA implantation are often not recognized intraoperatively, thus leading to fracture initiation during postoperative weight bearing. Loose femoral stems can trigger cortical thinning, especially at the tip of the stem.

Periprosthetic fractures are influenced by bone quality and the stability of stem fixation. They are often located around the tip of the stem, if it is well-fixed. These are classified as Vancouver type B1 as proposed by Duncan and Masri [3]. Accounting for 29 % of all periprosthetic femur fractures, type B1 fractures are the most common, most complex to manage and associated with most complications [4]. Type B1 fractures are treated by an internal fixation with preservation of the prosthesis stem [3, 5]. In many cases, Ogden-type construct variations are applied, where a metal plate, placed laterally on the femur, is fixed proximally with cerclage wires or cables and distally with bicortical screws [4].

Clinical results for the original Ogden plate with an overall complication rate up to 30 % are not encouraging [6]. The Mennen plate system (a clamp on plate) showed even poorer results with failure rates over 75 %, being not stable enough for such application [7]. Combinations of plate osteosynthesis with allograft struts can further improve stiffness [8]. However, this technique is not compatible with minimally invasive surgical techniques. The overall complication rate for this procedure was recently stated to be 24 % [9]. Several biomechanical studies assume advantages in axial and rotational stability for unicortical locking plate compared to the Ogden construct [10–12]. Unicortical locking plate failure is mainly due to pull out of the proximal unicortical screws [13].

Based on the concept of angulated locking screw positioning, a new prototype plate for periprosthetic fracture fixation (A-LCP) was developed. The aim of the current study was to investigate, whether the prototype plate (A-LCP) provides better stability and strength compared to the conventional locking compression plate (LCP).

Materials and methods

Twelve fresh frozen (−20 °C) cadaveric femora (6 pairs, 2 male, 4 female donors) were used. The specimens were thawed at room temperature 24 h prior to instrumentation, embedding and mechanical testing. Conventional anteroposterior and mediolateral radiographs were taken from all

specimens to confirm absence of preexisting pathology or prior fractures. Bone mineral density (BMD) was evaluated using peripheral quantitative computed tomography (pQCT, Densiscan 1000, SCANCO Medical AG, Bassersdorf, Switzerland). The region of interest for BMD measurement was defined as largest cross-sectional area in the femoral head perpendicular to the femoral neck axis plus three slices of 1 mm increment in each direction. BMD was evaluated over the whole cross-sectional area (cancellous and cortical bone) and computed as the mean value of all cross-sectional values (7 slices). Left and right femora were assigned randomly to either Group (LCP) or Group (A-LCP), allowing a pair wise comparison.

Cemented Charnley hip endoprostheses (DePuy, Warsaw IN, USA), size 40 or 45, dependant on the femur dimensions, were implanted into the specimens by an experienced surgeon (Steve Joseph) according to the manufacturer's instructions and cemented with a Polymethylmethacrylate (PMMA)-based cement (CMV-1®, DePuy, Warsaw IN, USA), prepared under vacuum and inserted under pressure. A cement restrictor was inserted 1 cm beyond the tip of the prosthesis prior to cement insertion. The position of the prosthesis was assessed radiographically. An osteotomy was set 10 mm distally to
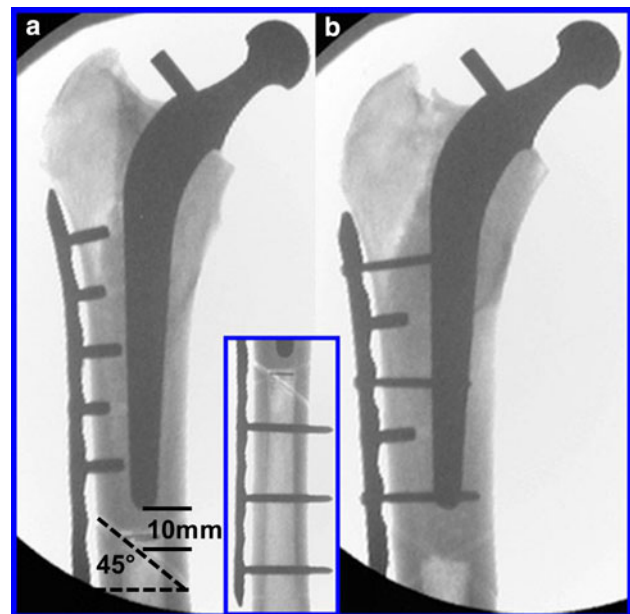

Fig. 1 Radiographs showing the osteotomized and instrumented femora of both study groups. **a** Conventional LCP plate with five unicortical proximal locking screws. The level of the osteotomy was determined radiographically after implantation of the prosthesis. The 45° osteotomy (*black dashed line*) oriented from proximal lateral to distal medial was set 1 cm distal to the tip of the prosthesis (*black lines*). **b** Angulated LCP plate with three 3.5 mm 30° dorsally angulated bicortical and two 5.0 mm straight monocortical locking screws. The insert shows the distal fixation being equally performed with three 5.0-mm bicortical screws in both study groups

the tip of the prosthesis at an angle of 45°, measured along the bone axis, from proximal lateral to distal medial (Fig. 1) to simulate a Vancouver type B1 periprosthetic fracture [3]. The osteotomy gap was closed before plate fixation to simulate a stable situation. In one study group (LCP), a 12-hole conventional broad LCP (Synthes GmbH, Solothurn, Switzerland) was used. Five unicortical 5.0 mm head-locking screws were applied for its proximal fixation and three bicortical 5.0 mm locking screws for the distal fixation. In the other study group (A-LCP), a prototype locking plate with design, based on that of the 12-hole conventional broad LCP, was used. During its development phase, possible corridor for posterior angulated bicortical locking screws proximally (at the level of the prosthesis stem) was determined by the use of computerized tomography (CT) scans of the femora with an implanted THA (Fig. 2). The CT scans revealed that anterior angulation would not be possible. That is why the prototype locking plate (A-LCP) was developed with 30° posterior angulation of the first, third and fifth proximal locking screws with 3.5-mm diameter (Fig. 3). The rest of its holes were identical to the respective angle-stable locking holes of the 12-hole conventional broad LCP, with additional two
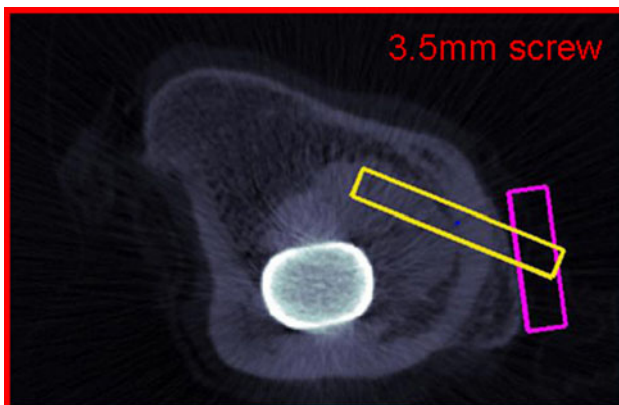

Fig. 2 Computed tomography scan of proximal femur with implanted hip endoprosthesis. Axial view, showing the position of the prosthesis stem within the femoral shaft and the femoral cortical circumference. Possible corridor for angulated bicortical screw position was determined and marked with *yellow rectangle*. *Blue rectangle* defines the position of the osteosynthesis plate

unicortical 5.0 mm screws for its proximal fixation. The distal fixation was identical to the LCP group with three bicortical 5.0 mm locking screws. All plates were anatomically pre-bent to fit exactly to the lateral femoral cortex and positioned with the two vacant holes over the osteotomy (number 6 and 7, counted from proximal to distal). Kirschner wires were positioned via drill sleeves into the three proximal angulated screw holes in the A-LCP group to fix the plate preliminary in an exact position, thus ensuring a strictly intraosseous bicortical angulated screw positioning. Care was taken not to screw into the cement mantle. Correct fitting of the instrumentation was assessed radiologically for each specimen (Fig. 1). The distal ends of all the specimens were embedded in polymethylmethacrylate (PMMA, SCS Beracryl®; W. Troller Kunststoffe AG, Jegenstorf, Switzerland) up to 5 mm distally to the plate. Prior to embedding, all exposed implant surfaces were covered with plasticine to prevent direct contact with the PMMA. The specimen axis was aligned along the femoral shaft axis. For fracture gap movement monitoring, an optical 3D motion tracking system with two marker sets of four retro-reflective markers each was mounted on the bone proximally and distally to the osteotomy site and aligned as required (Fig. 4).

Mechanical testing was performed on a servohydraulic mechanical test system (Mini Bionix 858; MTS Systems, Eden Prairie, MN, USA) with a 4 kN/20 Nm load cell. The specimens were attached to the test frame proximally via a ball and socket joint and distally via a cardan joint. They were kept moist during the test procedure. At the beginning and after 10,000 cycles, all specimens were loaded in axial bending with a quasi-static ramp from 50 to 500 N at a rate of 30 N/s, followed by a non-destructive quasi-static torsional test in internal rotation, simulating rising from a chair [14], ramped from 0.4 up to 3.0 Nm at a rate of 0.2 Nm/s. During the quasi-static tests, the femoral shaft axis was oriented vertically, in parallel to the machine axis with the cardan joint fixed. The cyclic mechanical test was performed at a rate of 2 Hz with synchronal sinusoidal axial loading at constant amplitude of 950 N during the first 10,000 cycles, keeping the axial forces in the range from 50 N (valley) to 1,000 N (peak). After 10,000 cycles, the valley load level was kept constant (50 N), while the
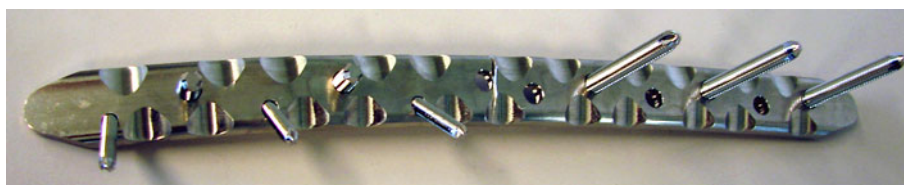

Fig. 3 Prototype plate developed for this study with three 30° dorsally angulated 3.5-mm locking screws and additional two unicortical 5.0-mm locking screws for proximal fixation and three bicortical 5.0-mm locking screws for distal fixation
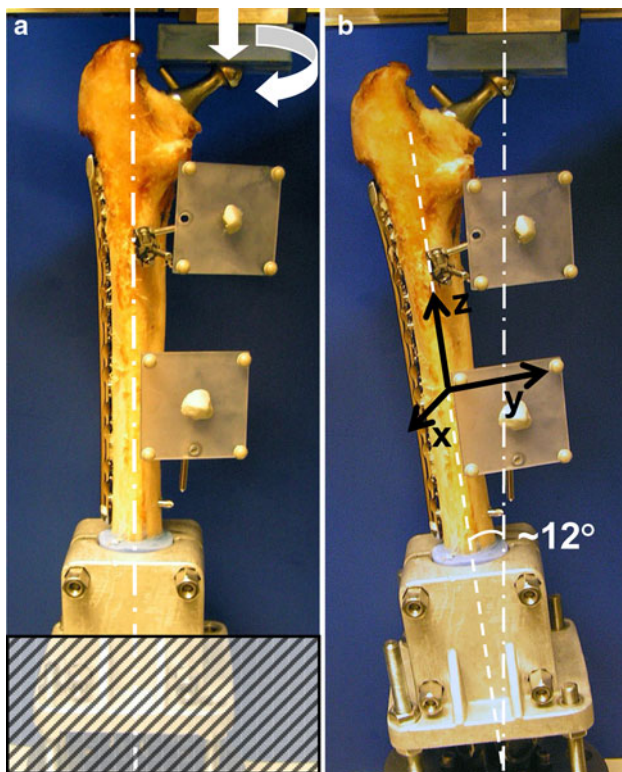
Fig. 4 Instrumented specimens with fixed retroreflective marker sets for motion tracking, mounted in the servohydraulic test system. The endoprosthesis head was part of the proximal ball and socket joint. Distally, the specimens were connected to the testing frame via a cardan joint. **a** For axial bending and torsional quasi static testing, the load axis was orientated along the femur shaft axis (*white dot* and *dash line*) and the distal cardan joint was fixed. **b** Cyclic testing was performed with the load axis in 12° valgus position (*white dot* and *dash line*), ensuring a physiological load bearing of the construct with axial compression force as main load. *Black arrows* indicate the defined Cartesian coordinate system linked to the distal femur fragment with the following features: center at the intersection of the distal border of the osteotomy gap and the central axis of the femur; z axis in the proximal direction along the central axis of the femur; and x axis in the posterior direction used to chart osteotomy gap movement

peak load level, starting from 1,000 N, was monotonically increased at a rate of 0.1 N/cycle until catastrophic construct failure occurred. Using continuously increasing peak load allowed comparison of cyclic testing data from specimens with different bone quality. The principle of cyclic testing with monotonically increasing peak load has proven to be useful in previous studies [15].

For cyclic testing, the weight bearing axis was orientated from the center of rotation of the hip joint (head of the prosthesis) to the center of the distal end of the PMMA pot, creating a valgus position of the bone, ensuring a physiological load bearing of the construct with axial compression force as main load (Fig. 4). According to the model of Duda et al. [16], considering muscle activity for calculation

of internal femoral forces and moments, axial compression is the main loading mode within the femoral shaft cortex during a gait cycle, while torsional moments, being relatively low, remain constant along the femoral shaft. Pure bending moments of the femoral shaft, alternating in direction, are only minimal. Therefore, the weight bearing axis was orientated as described above. Furthermore, this position simulates a one-legged stand [10], considered as worst case scenario for hip joint loading.

Axial load, axial displacement, torsional angle and torsional moment were recorded from the test system's transducers at a sampling rate of 128 Hz. At the beginning of the test and after 10,000 cycles, axial bending and torsional stiffness of the constructs were determined from the load–displacement curve of the machine data within the quasi-static ramp from 100 to 400 N and 1 to 2 Nm, respectively.

Relative movements at the osteotomy gap were measured optically in all six degrees of freedom with use of 3D motion tracking, monitoring the specimen marker sets with five digital cameras (ProReflex MCU; Qualisys AB, Gothenburg, Sweden) at a rate of 100 Hz. Both optical and machine data were captured simultaneously. Using the optical data, medial bending and axial translation were calculated as functions over time. For this purpose, a custom-made software (Matlab R2010a; The Mathworks, Natick, MA, USA) was used to define a Cartesian coordinate system linked to the distal femur fragment with the following features: Center at the intersection of the distal border of the osteotomy gap and the central axis of the femur; z axis in the proximal direction along the central axis of the femur; and x axis in the posterior direction (Fig. 4) [17]. Failure criterion was set at 2 mm relative movement in axial translation at the osteotomy gap. Radiographs were taken every 500 cycles during cyclic testing to detect the location of construct failure onset. Statistical analysis was performed with the use of SPSS software (IBM SPSS Statistics 19.0; SPSS Inc., Chicago, IL, USA). The significance of differences between the groups regarding the BMD, the osteotomy gap movement (axial translation and medial bending angle at cycle 5,000 and cycle 15,000) and cycles to failure during the cyclic test was determined with Mann–Whitney U test. Significance of differences between the two evaluation time points (cycle 1 and cycle 10,000) within the A-LCP and LCP group and between the A-LCP and LCP group within the same time points was detected with the Wilcoxon-signed-rank test. Significance level was defined as $p = 0.05$.

Results

The BMD was equally distributed between the two groups with a mean BMD of 0.306 g/cm^3 (range 0.268–0.339 g/cm^3

± 0.024 standard deviation (SD), $p = 0.31$). The axial bending stiffness and the torsional stiffness of the A-LCP group and the LCP group are shown in Table 1. The relative movements for bending in varus were significantly different between the two groups after 5,000 cycles (A-LCP 2.09° ± 0.57; LCP 5.02° ± 4.04; $p = 0.02$) and after 15,000 cycles (A-LCP 2.96° ± 0.70; LCP 6.52° ± 2.31; $p = 0.01$). The relative movements for translation in axial direction were significantly different between the groups after 5,000 cycles (A-LCP 1.25 mm ± 0.33; LCP 2.81 mm ± 2.32; $p = 0.02$) and after 15,000 cycles (A-LCP 1.68 mm ± 0.32; LCP 3.14 mm ± 0.68; $p = 0.01$).

The cycles to failure and the corresponding load to failure were significantly higher in the A-LCP group (15,500 ± 2,828; mean 1,550 N) compared to the LCP group (5,417 ± 7,236; mean 1,000 N), $p = 0.03$. The cumulative survival of both constructs up to the failure criterion of 2 mm axial displacement is shown in Fig. 5. In the radiographs, we observed in all specimens of both groups a blast of the medial cortical shell of the proximal fragment at the osteotomy, followed by a plate bending with concomitant distal failure or followed by a pullout failure of the proximal fragment. In both groups, total construct failure occurred mainly distal to the osteotomy gap, with a proximal to distal failure ratio of 1:5 in the A-LCP group and 2:4 in the LCP group (Fig. 6).

Fig. 5 Cumulative survival in both groups upon cycle number. Cumulative survival rate (y axis) is scaled from 100 % of the specimens intact down to 0 % of the specimens intact—all specimens failed. Failure criterion was defined as a relative movement of 2 mm in axial translation at the osteotomy gap

Discussion

Construct stability and strength could be improved by the A-LCP prototype plate, expressed in a significantly lower interfragmentary movement at the osteotomy gap in axial translation and medial bending and a significantly higher number of cycles to failure.

Nevertheless, predominant total proximal pullout failure in the LCP group did not occur as initially expected. In contrast to Konstantinidis et al., who observed proximal screw pullout failure [18], we used a fracture model with a closed osteotomy gap, transmitting the load also via the medial cortex. In our model, the load bearing axis is medial to the osteotomy as it would be in the normal human stand phase and the medial cortex acts as main axial load carrier transmitting the load distal to the osteotomy. Total failure occurred predominantly distally to the osteotomy gap after loss of medial cortical support and plate bending, emphasizing the importance of medial cortical support as load carrier in femoral shaft fracture fixation. The fracture model of Konstantinidis et al. has a 10-mm gap at the osteotomy, so that the plate acts as main load carrier in this section and no cortical support impeded axial translation of the proximal fragment along the plate [18]. Although the osteotomy gap was closed in our study, providing medial cortical support, we observed a significantly larger relative movement in axial translation and medial bending in the LCP group, indicating a higher elastic and plastic construct deformation. The relative movement is a criterion for the mechanical construct stability in experimental studies [19]. Under cyclic activity, a higher amount of load can be transferred via the A-LCP, providing an improved

Table 1 Axial bending stiffness (a) and torsional stiffness (b)

	A-LCP		LCP	
	0 cycles	10,000 cycles	0 cycles	10,000 cycles
(a) Axial bending stiffness (N/mm)				
Mean	1,633	1,368	1,402	1,029
SD	548	650	272	387
p value	0.12		0.08	
A-LCP-LCP	0 cycles		10,000 cycles	
p value	0.463		0.249	
(b) Torsional stiffness (in Nm/deg)				
Mean	0.75	0.67	0.54	0.45
SD	0.23	0.25	0.19	0.15
p value	0.17		0.03*	
A-LCP-LCP	0 cycles		10,000 cycles	
p value	0.05*		0.75	

Mean stiffness values with standard deviation (SD) of the A-LCP and LCP group at the beginning and after 10,000 cycles are shown including the p values of the comparisons between the time points (0 cycles, 10,000 cycles) for each group and between the groups at the different time points
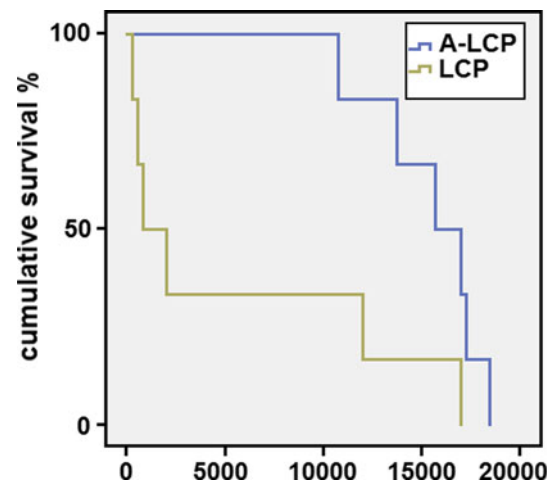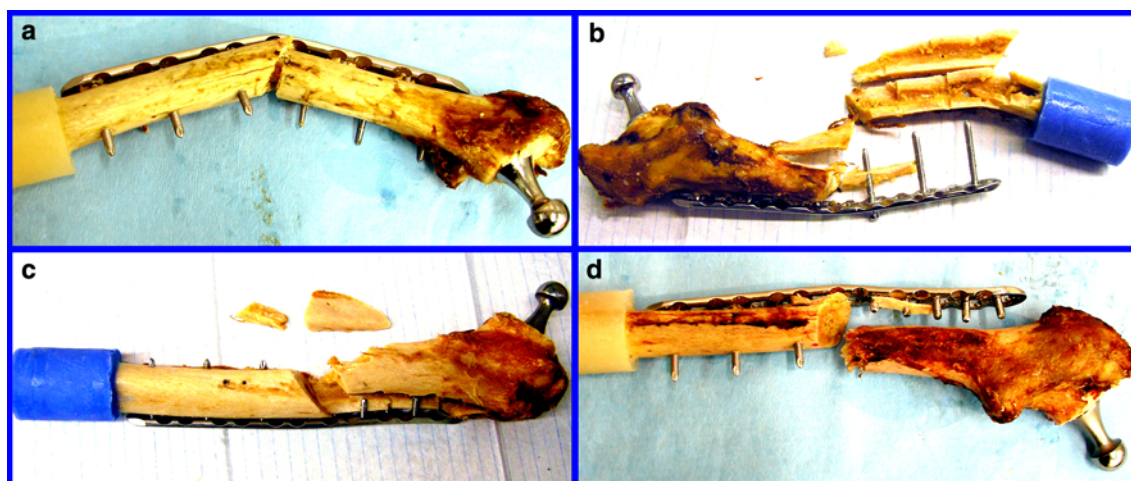
* Difference significant

Fig. 6 Failure modes. Both failure modes, proximal and distal failure occurred in both groups. Failure distal to the osteotomy was the preponderant failure mode in both groups. Angulated locking plate (A-LCP) exhibited a proximal to distal failure ratio of 1:5, whereas the failure ratio of the LCP group was 2:4. Failure distal to the osteotomy is shown in **a**, **b** for the A-LCP and failure proximal to the osteotomy in **c**, **d** for the LCP. Note that in all specimens, the medial cortical support at the osteotomy is lacking due to the blasted medial cortical shell of the proximal femoral part. Due to the lacking medial support, bending of the plate at the osteotomy occurred, provoking a shift of the load axis so that distal failure occurred (**a**, **b**). If the medial support lacks and plate bending is absent, proximal failure occurred (**c**, **d**)

proximal fixation to the femur and allowing less relative movement at the fracture gap.

We observed no significant difference in axial bending stiffness between both constructs, which is related to the lower load level (ramp to 500 N), where the stiffness was determined compared to the relative movements at the osteotomy gap, which were recorded under cyclic loading up to 1,000 N. A ramp to 500 N has been repeatedly used for non-destructive quasi-static axial loading in periprosthetic fracture fixation testing [8, 10, 11, 14, 19]. Many biomechanical studies use only quasi-static loading tests or loads far below physiologic levels [11–13]. To simulate real-life conditions, a cyclic test protocol with monotonically increasing load and increments per each cycle is recommended. In the current study, loading forces up to two to threefold body weight were barely achieved during cyclic testing before failure occurred. The constructs would just survive normal daily activity with load bearing of one to twofold body weight, excluding fast walking and going upstairs [20, 21]. The fact that using crutches can reduce the hip contact force to 1.8-fold body weight [20] is an important advice in this context. Correlating our results with the telemetric in vivo measurements of Bergmann et al., who recorded hip contact forces up to eightfold body weight during stumbling [22] explains the high failure rate of fixation of periprosthetic fractures. Several studies used load to failure tests in torsional loading [11, 14]. It is commonly accepted that certain hip prosthesis stems, particularly symmetric ones, are susceptible to torsional loading with maximal relative movements under this loading mode [23]. Further, torsional femoral loading is surmised in activities with the hip joint in flexion like rising from a chair [10]. On the other hand, current models of femoral loads and moments indicate quite small torsional moments during cyclic load bearing activities such as walking [16]. Hence, destructive cyclic testing should be performed in the modality where the main load occurs, which is axial loading for the femoral shaft. However, torsional stability is not dispensable particularly in stair climbing and fast walking as revealed in the in vivo measurements of Bergmann et al. [24]. Internal torsion of the stem is probably critical for stem fixation [24] due to relatively poor torsional stability of the stem. Therefore, torsional stability was tested in internal rotation with our test setup for quasi-static testing, though we only observed a significant difference in torsional stiffness between both constructs at the beginning of the test, but not after 10,000 cycles. Wilson et al. [25] observed in their biomechanical in vitro study on six cadaveric femora, tested with different plate-allograft fixation constructs, that fixation with proximal unicortical screws could significantly reduce interfragmentary movement under axial and torsional loading.

Bone quality is another important factor influencing osteosynthesis failure. Despite the mean BMD of 0.306 g/cm^3 for both groups in this study, which is relatively high with regard to osteoporosis, we were able to point out significant differences between the two groups in terms of relative osteotomy gap movements.

Talbot et al. tested 15 artificial femora with a type Vancouver B1 fracture biomechanically, fixed with

allograft strut in combination with locking plate or non-locking plate versus locking plate alone with unicortical proximal screws, showing that only bending stiffness and axial load to failure were improved to a certain degree using allograft struts [26]. The cyclic load to failure in their study was quite high (3,500–4,000 N) and should be interpreted with caution since artificial femora were used. The combination of allograft strut and plate effectively acts as a two-plate system with different elasticity modulus, thus providing three-dimensional stability of fixation. Due to its angulated locking screws, the angulated locking plate offers principally three-dimensional stability with improved stiffness compared to the conventional locking plate and with less soft tissue exposure during implantation in contrast to the allograft struts.

Comparing a locking to a conventional screw in plating, the former transmits forces over its whole length. Therefore, locking screws are ideal for bicortical fixation. Using straight locking screws, bicortical proximal screw fixation is impossible because the intramedullar space is already blocked by the prosthesis stem. The idea of the angulated screw concept is to combine the advantages of locking screws and bicortical proximal screw fixation. Kobbe et al. reported a series of 21 patients with periprosthetic fractures Vancouver type B and C, treated with the less invasive stabilization system (LISS), allowing angulated proximal screw positioning [27]. In their 3-year follow-up, they reported on a complication rate of 10 %, namely two implant failures. Kääb et al. published a series of 11 periprosthetic hip fractures stabilized with LISS plate where one implant failure and two malunions were observed [28]. Both studies demonstrated that good clinical results in periprosthetic fracture surgery could be obtained with bicortical locking screw plating.

Conclusion

Although the possible bone corridor for angulated screw positioning is narrow with this prototype implant, the bicortical locking screw placement adjacent to the prosthesis stem is an attractive option to enhance mechanical stability and strength in proximal plate fixation of periprosthetic femur fracture fixation. Beside the plate osteosynthesis, medial cortical support is considered as an important load carrier in femoral shaft fracture fixation.

References

1. Tsiridis E, Haddad FS, Gie GA (2003) The management of periprosthetic femoral fractures around hip replacements. Injury 34:95–105

2. Parvizi J, Rapuri VR, Purtill JJ, Sharkey PF, Rothman RH, Hozack WJ (2004) Treatment protocol for proximal femoral periprosthetic fractures. J Bone Joint Surg Am 86-A(Suppl 2):8–16

3. Duncan CP, Masri BA (1995) Fractures of the femur after hip replacement. Instr Course Lect 44:293–304

4. Ogden W, Rendall J (1978) Fractures beneath hip prostheses: a special indication for Parham bands and plating. Orthop Trans 2:70

5. Wilson D, Masri BA, Duncan CP (2001) Periprosthetic fractures: an operative algorithm. Orthopedics 24:869–870

6. Zenni EJ Jr, Pomeroy DL, Caudle RJ (1988) Ogden plate and other fixations for fractures complicating femoral endoprostheses. Clin Orthop Relat Res 231:83–90

7. Kamineni S, Ware HE (1999) The Mennen plate: unsuitable for elderly femoral peri-prosthetic fractures. Injury 30:257–260

8. Zdero R, Walker R, Waddell JP, Schemitsch EH (2008) Biomechanical evaluation of periprosthetic femoral fracture fixation. J Bone Jt Surg Am 90:1068–1077

9. Virolainen P, Mokka J, Seppanen M, Makela K (2010) Up to 10 years follow up of the use of 71 cortical allografts (strut-grafts) for the treatment of periprosthetic fractures. Scand J Surg 99:240–243

10. Dennis MG, Simon JA, Kummer FJ, Koval KJ, DiCesare PE (2000) Fixation of periprosthetic femoral shaft fractures occurring at the tip of the stem: a biomechanical study of 5 techniques. J Arthroplast 15:523–528

11. Fulkerson E, Koval K, Preston CF, Iesaka K, Kummer FJ, Egol KA (2006) Fixation of periprosthetic femoral shaft fractures associated with cemented femoral stems: a biomechanical comparison of locked plating and conventional cable plates. J Orthop Trauma 20:89–93

12. Lever JP, Zdero R, Nousiainen MT, Waddell JP, Schemitsch EH (2010) The biomechanical analysis of three plating fixation systems for periprosthetic femoral fracture near the tip of a total hip arthroplasty. J Orthop Surg Res 5:45

13. Schmotzer H, Tchejeyan GH, Dall DM (1996) Surgical management of intra- and postoperative fractures of the femur about the tip of the stem in total hip arthroplasty. J Arthroplast 11:709–717

14. Dennis MG, Simon JA, Kummer FJ, Koval KJ, Di Cesare PE (2001) Fixation of periprosthetic femoral shaft fractures: a biomechanical comparison of two techniques. J Orthop Trauma 15:177–180

15. Windolf M, Muths R, Braunstein V, Gueorguiev B, Hänni M, Schwieger K (2009) Quantification of cancellous bone-compaction due to DHS Blade insertion and influence upon cut-out resistance. Clin Biomech (Bristol, Avon) 24:53–58

16. Duda GN, Schneider E, Chao EY (1997) Internal forces and moments in the femur during walking. J Biomech 30:933–941

17. Gueorguiev B, Wahnert D, Albrecht D, Ockert B, Windolf M, Schwieger K (2011) Effect on dynamic mechanical stability and interfragmentary movement of angle-stable locking of intramedullary nails in unstable distal tibia fractures: a biomechanical study. J Trauma 70:358–365

18. Konstantinidis L, Hauschild O, Beckmann NA, Hirschmüller A, Südkamp NP, Helwig P (2010) Treatment of periprosthetic femoral fractures with two different minimal invasive angle-stable plates: biomechanical comparison studies on cadaveric bones. Injury 41:1256–1261

19. Moazen M, Jones AC, Jin Z, Wilcox RK, Tsiridis E (2011) Periprosthetic fracture fixation of the femur following total hip arthroplasty: a review of biomechanical testing. Clin Biomech (Bristol, Avon) 26:13–22

20. Bergmann G, Rohlmann A, Graichen F (1989) In vivo measurement of hip joint stress. 1. Physical therapy. Z Orthop Ihre Grenzgeb 127:672–679

21. Wirtz DC, Heller KD, Niethard FU (1998) Biomechanical aspects of load-bearing capacity after total endoprosthesis replacement of the hip joint. An evaluation of current knowledge and review of the literature. Z Orthop Ihre Grenzgeb 136:310–316

22. Bergmann G, Graichen F, Rohlmann A (2004) Hip joint contact forces during stumbling. Langenbecks Arch Surg 389:53–59

23. Hua J, Walker PS (1994) Relative motion of hip stems under load. An in vitro study of symmetrical, asymmetrical, and custom asymmetrical designs. J Bone Jt Surg Am 76:95–103

24. Bergmann G, Deuretzbacher G, Heller M, Graichen F, Rohlmann A, Strauss J, Duda GN (2001) Hip contact forces and gait patterns from routine activities. J Biomech 34:859–871

25. Wilson D, Frei H, Masri BA, Oxland TR, Duncan CP (2005) A biomechanical study comparing cortical onlay allograft struts and plates in the treatment of periprosthetic femoral fractures. Clin Biomech (Bristol, Avon) 20:70–76

26. Talbot M, Zdero R, Schemitsch EH (2008) Cyclic loading of periprosthetic fracture fixation constructs. J Trauma 64:1308–1312

27. Kobbe P, Klemm R, Reilmann H, Hockertz TJ (2008) Less invasive stabilisation system (LISS) for the treatment of periprosthetic femoral fractures: a 3-year follow-up. Injury 39:472–479

28. Kääb MJ, Stöckle U, Schütz M, Stefansky J, Perka C, Haas NP (2006) Stabilisation of periprosthetic fractures with angular stable internal fixation: a report of 13 cases. Arch Orthop Trauma Surg 126:105–110